Seed-Mediated Synthesis of Branched Gold Nanocrystals Derived from the Side Growth of Pentagonal Bipyramids and the Formation of Gold Nanostars

Hsin-Lun Wu, Chiu-Hua Chen, and Michael H. Huang*

Department of Chemistry, National Tsing Hua University, Hsinchu 30013, Taiwan

Received August 20, 2008. Revised Manuscript Received November 11, 2008

We report the first synthesis of elongated penta-branched gold nanocrystals with a shape resembling that of a star fruit but with sharp ends by a seeding growth approach. Cetyltrimethylammonium bromide (CTAB) capping surfactant was used, and $AgNO_3$ was added to the last growth solution to promote the formation of the five side branches. Through an investigation of the products collected by adding $AgNO_3$ into first, second, third, or fourth growth solution, the penta-branched nanocrystals were found to be derived from pentagonal bipyramid-shaped nanocrystals. Side growth over the twin boundaries results in the formation of five elongated branches with the highest point of each branch bisecting the branch into two halves. Smaller penta-branched nanocrystals with sizes of 70−110 nm and more fully developed larger nanocrystals with sizes of 200−350 nm can be readily prepared. The branches possess single-crystalline {111} faces. The intermediate products obtained at various time points were examined and their UV−vis absorption spectra recorded. By replacing CTAB with cetyltrimethylammonium chloride surfactant, and controlling the concentration of bromide ions in the solution, gold nanostars with five symmetrical branches and monodispersed sizes of 120−130 nm were synthesized for the first time.

Introduction

Research interests in the shape-controlled synthesis of gold nanostructures have resulted in the development of numerous methods for the growth of gold nanoparticles with various simple and symmetrical particle morphologies. However, for branched gold nanocrystals the particle morphology is often less well-controlled, and the number of branches or pods can vary within each preparation.[1−9] Thus, monopods, bipods, tripods, tetrapods, and other multipods can often be found in each sample. To synthesize branched gold nanocrystals with a specific number of branches, one may consider using structurally well-defined and multitwinned gold nanoparticles such as nanorods, bipyramids, and decahedra as templates or seeds for the overgrowth of branches. These nanocrystals possess 5-fold twinned structures; further growth of these particles may yield unusual penta-branched nanocrystals. Several reports have described the preparation and optical properties of gold pentagonal bipyramids.[10−14] Gold bipyramids are typically synthesized in a solution of $HAuCl_4$, ascorbic acid, capping surfactant, and $AgNO_3$. Gold seed particles are typically prepared and added to the reaction mixture to promote the growth of bipyramids, and $AgNO_3$ has also been found to be essential for their formation.[10−13] Although overgrowth of gold bipyramids has been observed, the products have more random morphologies.[14] A related penta-branched particle structure one can conceive has a star shape. Few studies have described their branched gold nanocrystals as possessing the star shape.[15−17] The nanostars have six or more pods, and the overall particle morphology is either symmetrical or distorted. However, gold nanostars with five branches have not been reported until recently by preparing them in a deep eutectic solvent.[18]

Here, we present the first seed-mediated synthesis of penta-branched gold nanocrystals derived from the side growth of pentagonal bipyramids. A small volume of a gold seed solution was added to a growth solution. Successive transfer of the growth solution to the next three growth solutions, and with the addition of $AgNO_3$ to the last growth solution, yields the penta-branched nanocrystals. The five branches

* To whom correspondence should be addressed. E-mail: hyhuang@mx.nthu.edu.tw.

(1) Nehl, C. L.; Hafner, J. H. *J. Mater. Chem.* **2008**, *18*, 2415.
(2) Xie, J.; Lee, J. Y.; Wang, D. I. C. *Chem. Mater.* **2007**, *19*, 2823.
(3) Chen, S.; Wang, Z. L.; Ballato, J.; Foulger, S. H.; Carroll, D. L. *J. Am. Chem. Soc.* **2003**, *125*, 16186.
(4) Hao, E.; Bailey, R. C.; Schatz, G. C.; Hupp, J. T.; Li, S. *Nano Lett.* **2004**, *4*, 327.
(5) Sau, T. K.; Murphy, C. J. *J. Am. Chem. Soc.* **2004**, *126*, 8648.
(6) Kuo, C.-H.; Huang, M. H. *Langmuir* **2005**, *21*, 2012.
(7) Wu, H.-Y.; Liu, M.; Huang, M. H. *J. Phys. Chem. B* **2006**, *110*, 19291.
(8) Yuan, H.; Ma, W.; Chen, C.; Zhao, J.; Liu, J.; Zhu, H.; Gao, X. *Chem. Mater.* **2007**, *19*, 1592.
(9) Bakr, O. M.; Wunsch, B. H.; Stellacci, F. *Chem. Mater.* **2006**, *18*, 3297.
(10) Liu, M.; Guyot-Sionnest, P. *J. Phys. Chem. B* **2005**, *109*, 22192.
(11) Kou, X.; Zhang, S.; Tsung, C.-K.; Yeung, M. H.; Shi, Q.; Stucky, G. D.; Sun, L.; Wang, J.; Yan, C. *J. Phys. Chem. B* **2006**, *110*, 16377.
(12) Kou, X.; Ni, W.; Tsung, C.-K; Chan, K.; Lin, H.-Q.; Stucky, G. D.; Wang, J. *Small* **2007**, *3*, 2103.
(13) Jana, N. R.; Gearheart, L.; Obare, S. O.; Murphy, C. J. *Langmuir* **2002**, *18*, 922.
(14) Zhang, X.; Tsuji, M.; Lim, S.; Miyamae, N.; Nishio, M.; Hikino, S.; Umezu, M. *Langmuir* **2007**, *23*, 6372.
(15) Yamamoto, M.; Kashiwagi, Y.; Sakata, T.; Mori, H.; Nakamoto, M. *Chem. Mater.* **2005**, *17*, 5391.
(16) Nehl, C. L.; Liao, H.; Hafner, J. H. *Nano Lett.* **2006**, *6*, 683.
(17) Burt, J. L.; Elechiguerra, J. L.; Reyes-Gasga, J.; Montejano-Carrizales, J. M.; Jose-Yucaman, M. *J. Cryst. Growth* **2005**, *285*, 681.
(18) Liao, H.-G.; Jiang, Y.-X.; Zhou, Z.-Y.; Chen, S.-P.; Sun, S.-G. *Angew. Chem., Int. Ed.* **2008**, *47*, 9100.

10.1021/cm802257e CCC: $40.75
Published on Web 12/09/2008

Scheme 1. Schematic Illustration of the Experimental Procedure Used to Make the Penta-Branched Gold Nanocrystals; Colors Shown Represent the Final Colors Observed for These Solutions

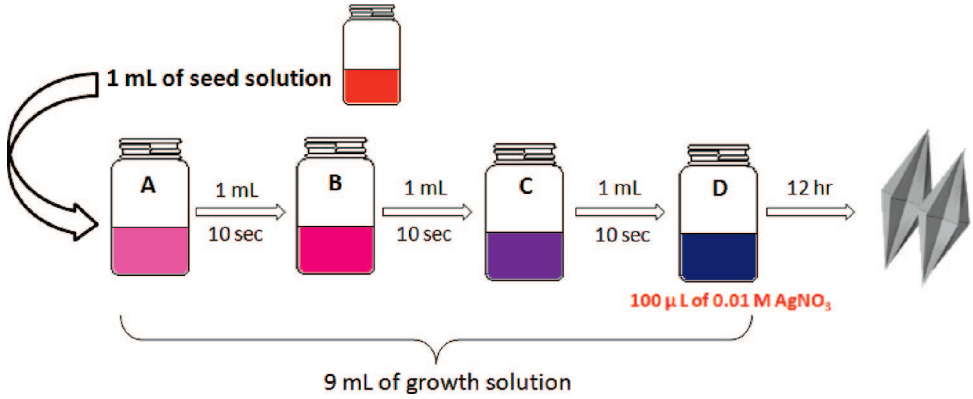

grow into a sheetlike or leaflike structure along the long axis of the bipyramid. We monitored the continuous formation of these penta-branched nanocrystals by examining the products formed at various time points. Experiments with $AgNO_3$ added to the first, second, third, or fourth growth solution were performed to show the necessity of this procedure for the preparation of well-developed penta-branched nanocrystals. Another interesting aspect of this work is the discovery of the facile synthesis of star-shaped gold nanocrystals with five branches. The concentration of bromide ions in the solution was found to be effective in regulating the formation of either nanostars or penta-branched nanocrystals.

Experimental Section

Synthesis of Gold Seeds. A volume of 0.2 mL of 0.025 M trisodium citrate solution was added to 19.8 mL of aqueous solution containing 2.5×10^{-4} M $HAuCl_4$. Concurrently, 20 mL of 0.01 M $NaBH_4$ solution was prepared by adding $NaBH_4$ to 20 mL of ice-cold 0.025 M trisodium citrate solution. When 0.6 mL of the $NaBH_4$ solution was added to the $HAuCl_4$ solution with stirring, the mixture gradually turned orange-red, indicating the formation of gold particles. All reagents were obtained from Aldrich.

Synthesis of Bipyramid-Derived Branched Gold Nanocrystals. In a typical synthesis, four 20 mL vials labeled A−D were used. A growth solution of sufficient volume was prepared containing 2.5×10^{-4} M $HAuCl_4$ and 0.10 M cetyltrimethylammonium bromide (CTAB) surfactant. To each of these vials was added 9.0 mL of growth solution. Then, 100 μL of 0.01 M $AgNO_3$ was introduced to solution D. Finally, 50 μL of 0.08 M ascorbic acid was added to each vial and the solution color turned colorless, indicating the reduction of Au^{3+} to Au^{+} species. Next, 1.0 mL of the gold seed solution was transferred to vial A. After being stirred for 10 s, 1.0 mL of the solution in vial A was withdrawn and added to vial B. The same transfer procedure was repeated twice more (from vial B to C and C to D). The colorless solution in vial D slowly turned blue. After reaction for 12 h at 30 °C, the solution was centrifuged at 1500 rpm for 10 min (Hermle Z323 centrifuge). Scheme 1 illustrates the experimental procedure.

Using a similar procedure as described above, bipyramid-shaped gold nanoparticles and smaller penta-branched gold nanocrystals can also be synthesized. Bipyramids can be prepared by adding 100 μL of 0.01 M $AgNO_3$ to the solution in vial B. There is no need for vials C and D. To make smaller penta-branched gold nanocrystals, 100 μL of 0.01 M $AgNO_3$ was added to the solution in vial C. Again vial D is not necessary. Vials B and C gradually turned purplish red and purplish blue, respectively. After reaction for 12 h at 30 °C, the solutions were, respectively, centrifuged at 4500 rpm for 10 min and 3500 rpm for 10 min to collect the products.

Synthesis of Star-Shaped Gold Nanocrystals. Again, four 20 mL vials labeled A−D were used. To each of these vials was added 9.0 mL of growth solution containing 2.5×10^{-4} M $HAuCl_4$, 0.10 M cetyltrimethylammonium chloride (CTAC), and 0.01 M NaBr. Then 100 μL of 0.01 M $AgNO_3$ was added to vial D. Lastly, 50 μL of 0.08 M ascorbic acid was introduced into each vial and the solutions turned colorless. Similarly, 1 mL of the gold seed solution was added to vial A. After 10 s, 1.0 mL of the solution in vial A was transferred to vial B. The procedure was repeated twice more (from vials B to C and C to D). The colorless solution also slowly turned blue. After reaction for 12 h at 30 °C, the solution in vial D was centrifuged at 1500 rpm for 10 min to collect the products.

Instrumentation. Transmission electron microscopy (TEM) images were acquired by using JEOL 2000FX and JEOL JEM-2010 microscopes with an operating voltage of 200 kV. Scanning electron microscopy (SEM) characterization of the samples was performed on a JEOL JSM-7000F electron microscopy. UV−vis absorption spectra were taken by using a JASCO V-570 spectrophotometer. X-ray diffraction (XRD) patterns of the samples were collected by using a Shimadzu XRD-6000 X-ray diffractometer with Cu Kα radiation.

Results and Discussion

The gold seeds were characterized to verify their sizes (see the Supporting Information). UV−vis absorption spectrum of the gold seed solution shows a single absorption band at ~510 nm. High-resolution TEM images reveal that the gold seeds are 2−5 nm in diameter. Lattice fringes are observable. A *d*-spacing of 2.36 Å was measured, which should correspond to the (111) lattice planes of gold.

The optimal preparation procedure for the synthesis of penta-branched gold nanocrystals is established after a series of seeding growth experiments with $AgNO_3$ added to different growth solutions. The corresponding control experiments without the addition of $AgNO_3$ were also conducted. Figure 1 shows the TEM images of the samples obtained with and without the addition of 100 μL of 0.01 M $AgNO_3$ into the growth solution in vial A, B, C, or D. Ellipsoidal nanoparticles with sizes of largely 10−15 nm were formed when $AgNO_3$ was added to vial A (Figure 1a). No other vials containing growth solution were used. Twin boundaries

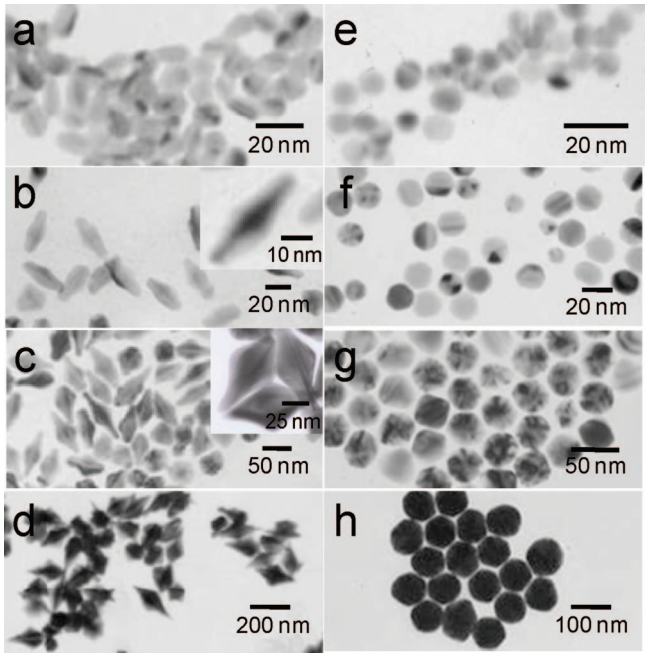

Figure 1. (a−d) TEM images of the products formed by adding 100 μL of 0.01 M $AgNO_3$, respectively, into the growth solution in vial A, B, C, or D. The insets show the enlarged TEM images. (e−h) Corresponding TEM images of the nanoparticles formed without the addition of $AgNO_3$ into the respective growth solution.

along the long axis of the particles can be seen. By introducing $AgNO_3$ into vial B, bipyramid-shaped gold nanoparticles with sizes of mostly 35−40 nm were produced (Figure 1b). The particle appearance is similar to that of reported pentagonal bipyramids, but with more rounded tips. Again the presence of twin boundaries running along the long axes of the bipyramids is discernible. Some particles exhibit slight protrusions near the middle portion. By adding $AgNO_3$ into vial C, penta-branched gold nanocrystals start to appear (Figure 1c). Their sizes roughly range between 70 and 110 nm, and the branches can be clearly distinguished. Some particles still do not have distinct side branches. To obtain penta-branched gold nanocrystals with fully developed branches and improve the yield, the standard procedure was employed with $AgNO_3$ solution added to vial D. The majority of the nanoparticles exhibit a penta-branched structure, and their sizes have increased to 200−350 nm (Figure 1d). Without the addition of $AgNO_3$, only highly faceted gold nanoparticles with increasing sizes were produced, a result similar to our previous study on the synthesis of faceted gold nanoparticles by the seeding growth approach (Figure 1e−h).[19] The control experiments demonstrate the importance of $AgNO_3$ for the formation of the penta-branched nanocrystals. The measured mean particle diameters for these samples are 6.9 ± 1.2, 18.7 ± 1.7, 34.2 ± 2.2, and 82.6 ± 4.4 nm.

Further structural characterization of the penta-branched gold nanocrystals was carried out on the samples with $AgNO_3$ solution added to vial D, since the branches are more completely formed. SEM images of the bipyramid-derived penta-branched nanocrystals clearly show the branches extending from the middle section out to the two tips (images

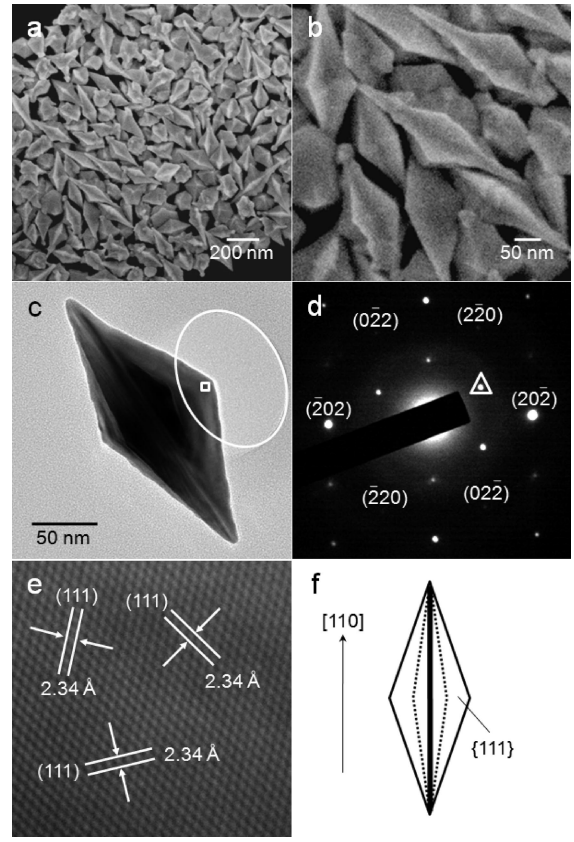

Figure 2. (a, b) SEM images of the penta-branched gold nanocrystals at different magnifications. (c) TEM image of a single penta-branched gold nanocrystal. (d) SAED pattern of the circled area in panel c. (e) High-resolution TEM image of the square region in panel c. (f) A model of the branched nanocrystal. The growth direction of [110] is the same as that of the penta-twinned gold nanorods.

a and b in Figure 2). The shape of each branch also reflects its origin from a pentagonal bipyramid, with the highest point of the branch bisecting the two halves of the branch. The morphology of these nanocrystals somewhat resembles that of a star fruit, or carambola, but with sharp ends. Thus, they may also be called star fruit-shaped gold nanocrystals. Interestingly, some particles contain spherical tips. This feature may be related to the presence of more rounded ends for the bipyramids. The XRD pattern of the penta-branched nanocrystals matches with that of face-centered cubic gold (see the Supporting Information). The (111) reflection peak is particularly strong in intensity relative to the other peaks, as is usually the case for gold nanostructures. Figure 2c is a TEM image of a single star fruit-shaped gold nanocrystal. Further confirmation of the possession of five branches was performed by a sample tilting experiment (see the Supporting Information). Figure 2d gives the selected-area electron diffraction (SAED) pattern of the circled region in panel c. The diffraction spots show a hexagonal pattern, and verify that each branch contains single-crystalline {111} faces similar to those of gold nanoplates.[20] The diffraction spot inside the marked triangle is attributed to the formally forbidden 1/3{4$\bar{2}\bar{2}$} reflections resulting from the thin plate structure.[21] The direction along the long axis is found to be

(19) Kuo, C.-H.; Chiang, T.-F.; Chen, L.-J.; Huang, M. H. *Langmuir* **2004**, *20*, 7820.

(20) Chu, H.-C.; Kuo, C.-H.; Huang, M. H. *Inorg. Chem.* **2006**, *45*, 808.

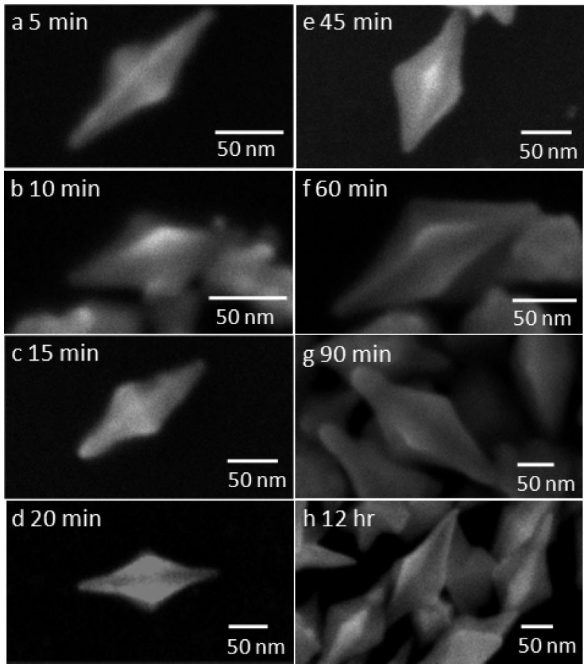

Figure 3. SEM images of the intermediate products observed by collecting the nanocrystals formed after reaction for 5, 10, 15, 20, 45, 60, and 90 min. Panel h shows the fully developed penta-branched nanocrystals formed after reaction for 12 h.

the [110] direction. Figure 2e displays the high-resolution TEM image of the square region of the branch shown in panel c. Three sets of lattice fringes with *d*-spacing of 2.34 Å were measured, and should correspond to the (111) lattice planes of gold. A schematic model of the branched nanocrystal is presented in Figure 2f.

The formation mechanism of the penta-branched nanocrystals was investigated by removing drops of the solution during the reaction for SEM analysis and measuring the UV−vis absorption spectra of the solution at various time points. Figure 3 provides the SEM images of the intermediate products observed. Because the initial particle concentration in the extracted drops is low, only one representative nanoparticle is shown for these time points. Pentagonal bipyramid-shaped nanocrystals with sizes of ∼150 nm are formed just 5 min after the reaction. Tiny protrusions near the middle section are visible. The particle size increases slightly to ∼180 nm after 1 h of reaction, but the branches have become fully developed much earlier. After the first hour, the branched nanocrystals show a more substantial increase in their sizes to 230−240 nm. Wider branches are observed for the 12 h nanocrystals. Figure 4 gives the UV−vis absorption spectra of the solution taken at different time points. The absorbance increases progressively indicating continuous formation of the branched gold nanocrystals. Within the first hour of reaction, the absorption profile consists of an absorption band at approximately 600 nm, a shoulder band at 550 nm, and a long tail into the near-infrared (near-IR) region. The bands at 550−600 nm should be attributed to the transverse absorption modes of the star fruit-

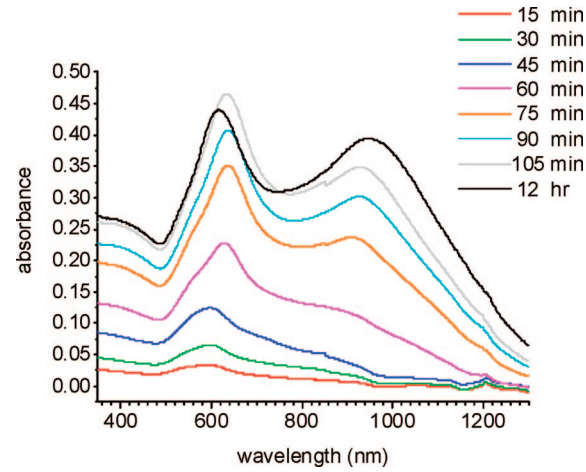

Figure 4. UV−vis absorption spectra of the intermediate products formed after different reaction times.

shaped nanocrystals with sheetlike branches if one considers the branched nanocrystals as a structural variation of the gold nanorods. Alternatively, the absorption band at 600 nm is related to the absorption modes of the branches with sheetlike or platelike morphology. The absorption band position at 600 nm is reminiscent of the approximate band position for thin gold nanoplates with widths of 40−60 nm.[22] The transverse absorption mode of the less-protruded portions (the regions between the branches) is believed to result in the appearance of the shoulder band at 550 nm. The near-IR absorption is due to the longitudinal absorption mode of the branched nanocrystals. After 1 h of reaction, the position of the shoulder band stays at ∼550 nm, but the 600 nm band has red-shifted to 640 nm. Evidently the significant shift in the transverse absorption band arises from the formation of fully developed side branches, as verified by the TEM images shown in Figure 3. The shoulder band remains fixed in position because growth in the regions between the branches is less obvious. The longitudinal absorption band becomes apparent, and gradually red-shifts from 910 to 940 nm. This shift is likely due to the elongation of the fully developed branched nanocrystals. After the completion of reaction, the two major absorption peaks locate at 620 and 960 nm.

From these observations and the results presented in Figure 1, the penta-branched gold nanocrystals are presumably derived from the side growth of initially formed pentagonal bipyramids. A schematic drawing illustrating the formation of the star fruit-shaped nanocrystals through the side growth and elongation of the particle length is available in the Supporting Information. Each of the five twin boundaries along the sides of a pentagonal bipyramid develops a branch. The fastest side growth appears to be near the middle section. Ag atoms are likely to deposit preferentially on certain sites or randomly on the surface of the pentagonal bipyramids.[10,14] With a rapid supply of more gold source in this seeding growth process and the assistance of silver atoms to promote the formation of bipyramids, a fast anisotropic crystal growth occurs, leading to the formation of side branches and finally the star fruit-shaped nanocrystals. The deposition of Ag

(21) (a) Jin, R.; Cao, Y.; Mirkin, C. A.; Kelly, K. L.; Schatz, G. C.; Zheng, J. G. *Science* **2001**, *294*, 1901. (b) Sun, Y.; Xia, Y. *Adv. Mater.* **2003**, *15*, 695.

(22) Huang, W.-L.; Chen, C.-H.; Huang, M. H. *J. Phys. Chem. C* **2007**, *111*, 2533.

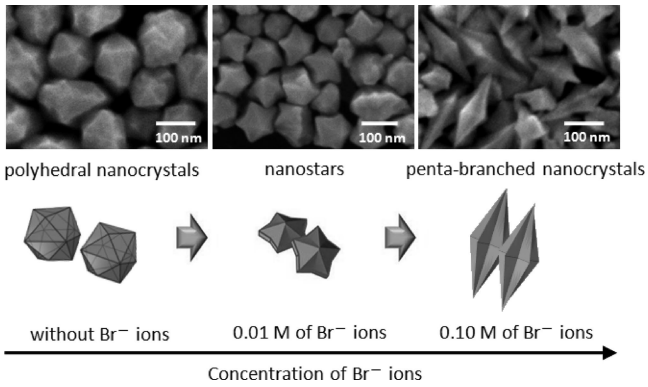

Figure 5. Shape evolution from polyhedral gold nanocrystals to nanostars and penta-branched nanocrystals with increasing bromide ion concentration in the reaction solution. For the synthesis of gold nanostars, 100 μL of 0.01 M $AgNO_3$ was also added to vial D.

atoms on the gold particle surface or incorporation into the gold lattice is favored over the influence of possible AgBr and AgCl deposition, since Au−Ag core−shell nanostructures can be readily synthesized, and AgBr and AgCl deposition cannot satisfactorily explain the formation of the five sheetlike branches.[23−25] Furthermore, the possibility of nitrate ions inducing the branch growth is ruled out, as replacing $AgNO_3$ with HNO_3, $NaNO_3$, and $Cu(NO_3)_2$ all resulted in the formation of polyhedral particles with sizes of about 100 nm (data not shown).

In an effort to reduce the sharp ends of the penta-branched nanocrystals, we discovered that gold nanostars can be prepared by adjusting the bromide ion concentration in the solution. To better control the concentration of Br^- ions, CTAB was replaced with CTAC surfactant, and NaBr was added to make the bromide ion concentration in the growth solution be 0.01 M. The same amount of $AgNO_3$ as that used to make the penta-branched gold nanocrystals (that is, 100 μL of 0.01 M $AgNO_3$) was added to vial D. Figure 5 illustrates the changes in the product morphology as a function of Br^- ion concentration. Additional SEM images of the nanostars are available in the Supporting Information. Although many nanoparticles still do not exhibit a well-defined star shape, the yield of nanostars is considerably high. Without Br^- ions in the growth solution, many irregularly shaped polyhedral nanocrystals with sizes of 100 nm or larger were produced. The gold nanostars synthesized have five symmetrical branches and monodispersed sizes of 120−130 nm. Twin boundaries bisecting each branch can be clearly seen. The nanostars are likely to form through the side growth of decahedra along the twin boundaries. Reducing the bromide ion concentration here appears to promote the side branch growth while inhibits the elongation of the nanocrystals. Due to their thickness and orientation problems, detailed TEM and SAED characterization was not so successful. Figure 6 presents the UV−vis absorption spectra of the three types of gold nanostructures shown in Figure 5. The nanostars display a single absorption band centered at 590 nm, and a long tail extending to the near-IR region. The lack of a prominent longitudinal absorption band reflects the presence of short branches and a thick body.

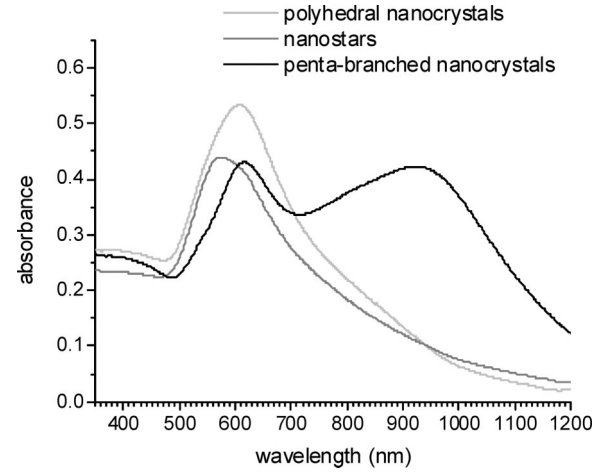

Figure 6. UV−vis absorption spectra of the polyhedral gold nanocrystals, nanostars, and penta-branched nanocrystals.

Conclusion

In summary, we have developed a simple seed-mediated growth approach to synthesize penta-branched gold nanocrystals which resemble the shape of a star fruit but with sharp ends. Through an examination of the products obtained by adding $AgNO_3$ into first, second, third, or fourth growth solution, the penta-branched nanocrystals were found to be derived from pentagonal bipyramid-shaped nanocrystals. Side growth over the twin boundaries results in the formation of five elongated branches. Silver ions are critical to promoting the development of side branches. The intermediate products collected at different time points during the reaction were also analyzed. By replacing CTAB with CTAC surfactant, and controlling the concentration of bromide ions in the solution, gold nanostars with five symmetrical branches were prepared for the first time. The penta-branched gold nanocrystals and nanostars represent a new class of branched gold nanostructures with well-defined particle morphologies throughout the sample. These novel gold nanostructures should offer opportunities for detailed analysis of their optical properties and applications in molecular sensing.

Acknowledgment. Financial support for this work is provided by the National Science Council of Taiwan (Grant NSC95-2113-M-007-031-MY3).

Supporting Information Available: Characterization of the gold seeds, XRD pattern of the penta-branched gold nanocrystals, sample-tilting TEM images of a single penta-branched nanocrystal, schematic drawing of the formation of penta-branched nanocrystals, and additional SEM images of the gold nanostars. This material is available free of charge via the Internet at http://pubs.acs.org.

CM802257E

(23) Fan, F.-R.; Liu, D.-Y.; Wu, Y.-F.; Duan, S.; Xie, Z.-X.; Jiang, Z.-Y.; Tian, Z.-Q. *J. Am. Chem. Soc.* **2008**, *130*, 6949.
(24) Tsuji, M.; Miyamae, N.; Lim, S.; Kimura, K.; Zhang, X.; Hikino, S.; Mishio, M. *Cryst. Growth Des.* **2006**, *6*, 1801.
(25) Pande, S.; Ghosh, S. K.; Praharaj, S.; Panigrahi, S.; Basu, S.; Jana, S.; Pal, A.; Tsukuda, T.; Pal, T. *J. Phys. Chem. C* **2007**, *111*, 10806.